The Sixth International Workshop on Micro and Nanotechnology for Power Generation and Energy Conversion Applications, Nov. 29 - Dec. 1, 2006, Berkeley, U.S.A.

A one-shot micro-valve with temperature dependent operation

A. Debray,[1,*] M. Shibata,[1] and H. Fujita[2]

[1] *Canon Inc., Canon Research Center 3-30-2, Shimomaruko, Ohta-ku, Tokyo 146-8501, Japan*

[2] *CIRMM, IIS, The University of Tokyo 4-6-1, Komaba, Meguro-ku, Tokyo 153-8505, Japan*

Abstract

A novel one-shot valve made using MEMS (Micro-Electro-Mechanical System) technologies has been designed, fabricated and characterized. The operation of the device is temperature dependent. It consists in a channel obstructed by a part made of a low melting point alloy. The valve is normally-closed and opens when the ambient temperature is higher than the melting temperature of the alloy. The device has been tested for several characteristics. It can withstand pressures up to 24 MPa in the closed state. Its leakage rate is below 2×10^{-10} mol.s^{-1} which is the limit of our measurement system and its temperature sensitivity is better than 3 °C. This device can have applications in small systems which require gas handling such as portable fuel cells or mini rockets for example.

Keywords: environment, temperature actuated, micro-valve, release valve, fuel cell

I. INTRODUCTION

By designing devices which simultaneously sense environmental parameters and act on a system, it is possible to avoid a complex aggregation of sensors, controllers and actuators. This solution is usually achieved by using 'smart materials'. Several examples using hydrogels and MEMS (Micro-Electro-Mechanical System) technologies have been reported [1–3]. These include micro-valves and micro-lenses which are sensitive to the pH, temperature or glucose concentration of a surrounding medium. Other materials have also been used to fabricate one-shot micro-valves. For example, Griss *et al* have used expandable micro-spheres to fabricate normally-open one-shot micro-valves [4]. Above 60 °C, the micro-spheres expand and obstruct a channel in which they are enclosed. In the macro-world, low melting point alloys are commonly used for one-shot valves, either for safety purpose or assembly [5, 6]. A channel is obstructed by the low melting point alloy which liquefy above its melting temperature, therefore releasing the channel under the action of a pressure difference. In this paper, we present a micro-version of these devices. The down-sizing allows to include the device into portable gas systems such as portable fuel cells, mini rockets or mini gas turbines.

II. DESIGN

The basic design of the device is similar to the macroscopic devices presented in the introduction. A scheme of the cross-section of the device in the closed state is shown in Fig. 1. The total dimensions of the device are $3 \times 3 \times 0.3$ mm^3. It consists in a silicon wafer perforated through its thickness by a channel. The channel is obstructed on its top by chromium and copper layers on which a low melting point alloy is fixed. The channel is circular with a radius of 50 or 100 μm. The alloy part possesses a square base from 300 to 600 μm width depending on the devices. Its height is typically around 80 μm.

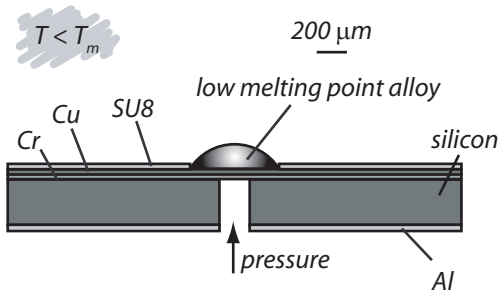

FIG. 1: Scheme showing the cross-section of the device in the closed position; T_m is the melting temperature of the low melting point alloy; T is the ambient temperature.

The working principle of the device is as follows. A scheme of the cross-section of the device in the opening position is shown in Fig. 2. When the ambient temperature is below the melting temperature of the alloy, this last is solid. The alloy part is therefore a thick, rigid part adhering to the silicon wafer via the chromium and copper layers. As a result it presents a high resistance to pressure differences across the channel and a low leakage rate. When the ambient temperature is above the melting temperature of the alloy, this last becomes liquid. The resistance to pressure differences is therefore determined

*Contact Author: debray.alexis@canon.co.jp

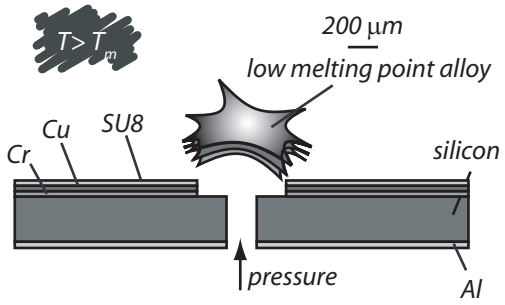

FIG. 2: Scheme showing the cross-section of the device while opening; T_m is the melting temperature of the low melting point alloy; T is the ambient temperature.

by the one of the chromium and copper layers and is far lower than that of the thick alloy part.

III. FABRICATION

The fabrication process starts with a 300 μm thick double-side polished silicon wafer. An aluminum layer is thermally deposited on the back-side and patterned by photo-lithography and metal etching (Fig. 3-a). This aluminum layer is to serve as a mask for deep-RIE (Reactive Ion Etching). On the front side, chromium and copper layers (around 200 nm thick each) are deposited by sputtering (Fig. 3-b). By using a 2 μm thick su8 photo-resist (su8-2, Microchem), the copper layer is covered except on a square pattern centered with the pattern of the channel (Fig. 3-c). Using the aluminum layer on the backside, a channel is etched all-through the thickness of the wafer by using deep-RIE (Fig. 3-d). The wafer is then dipped into a beaker containing two phases: on the bottom, the melted alloy and on the top, diluted HCl (pH $\sim$ 1). The alloy is composed of Bi, Sn, Pb, Cd and In with a melting temperature of 47 °C (LMA-117, Small Parts, Inc.). The temperature of the solution is kept at 55 °C. The diluted HCl etches the copper oxide naturally present at the surface of the copper layer. Due to the different interface tensions of the solder and the materials of the sample (su8, silicon and aluminum), the solder only coats the copper parts (Fig. 3e). This process is detailed in [7]. Each sample is then separated from the wafer.

Results from the fabrication process are presented in Fig. 4. Fig. 4-a shows a quarter of 3 inch wafer after fabrication on which most of the copper parts are coated with the alloy. Fig. 4-b shows a SEM micrograph of a cross-section of one device. The maximum height of the alloy part is around 80 μm. Fig 4-c and d show the device in the closed and open positions respectively. The open position shows remaining alloy on the copper layer as well as the channel clearly released. The device was opened

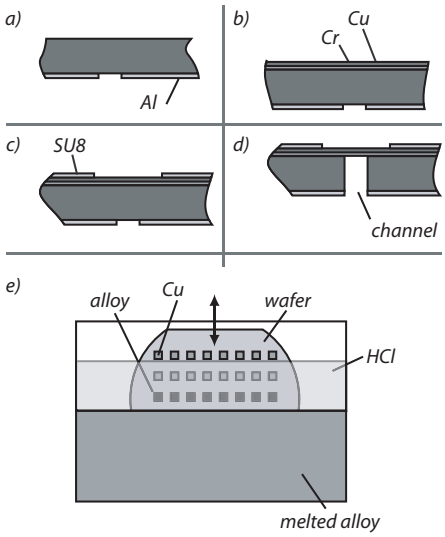

FIG. 3: Illustration of the fabrication process. a) Aluminum deposition and patterning; b) Chromium and copper deposition; c) Su8 deposition and patterning; d) Etching of the channel; e) Low melting point alloy deposition.

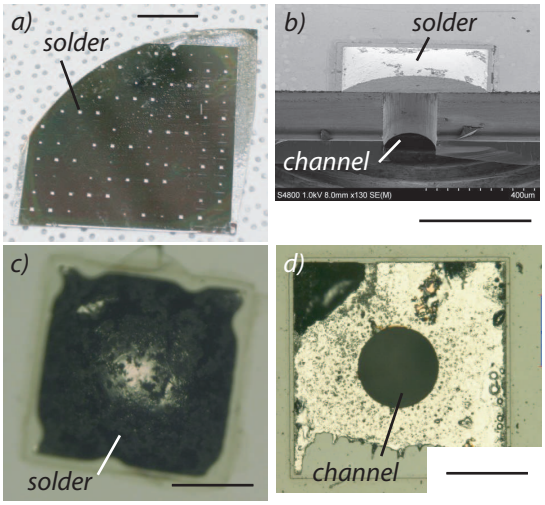

FIG. 4: a) Front side of a quarter of 3 inch wafer after fabrication. The alloy parts are clearly seen. Bar length is 1 cm; b) SEM micrograph of the cross section of one device. Bar length is 400 μm; c) Optical micrograph of the front side of one device in the closed position. Bar length is 200 μm; d) Optical micrograph of the front side of one device after being opened. Bar length is 200 μm.

at 60 °C with a pressure difference of 2.5 $\times 10^5$ Pa.

IV. EXPERIMENTAL CHARACTERIZATIONS

Several characteristics of the device have been evaluated experimentally. The design of the experimental set-up is

basically similar to the one reported in [8]. However, in these experiments, the experimental set-up is placed into a chamber which temperature and relative humidity are controlled. All the measurements have been performed with a relative humidity of 50 %.

A. Leakage rate

The leakage rate is measured using the VΔP method which consists in monitoring the pressure decay of a constant volume of gas connected to the device [9]. The measurements are performed with hydrogen which, because of its low molar mass (2 g.mol^{-1}), is a good choice to measure tiny physical leaks. The leakage rate of the device for a pressure difference of 2×10^5 Pa is found to be similar to the leakage rate of the packaging and is 2×10^{-10} mol.s^{-1}, which corresponds to 7 years per liter of hydrogen. The leakage rate of the device is therefore below this value and is better than most of those of previously reported micro-valves [8]. The experimental set-up needs to be improved to investigate further the leakage rate.

B. Maximum pressure

It is important to know the maximum pressure which can be withstood by the device in the closed state as this device can serve as a safety valve for high pressure tanks. The maximum pressure that can be withstood by the device is related to the force applied on the solder by the gas:

$$F_g = \Delta P \pi R_c^2, \tag{1}$$

and the force of adhesion of the chromium layer to the silicon wafer:

$$F_a = \alpha \left(W_a^2 - \pi R_c^2 \right), \tag{2}$$

with ΔP, the pressure difference across the channel, R_c the radius of the channel, α the adhesion coefficient of the chromium layer to the silicon wafer and W_a the width of the alloy part.

A tungsten wire (2 mm long and 120 μm in diameter) connected to a traction machine is introduced into the channel and pushes the alloy part until rupture. The maximum force before the chromium layer is detached from the silicon wafer is 0.77 N. Using the geometry of the device and equations 1 and 2, it is possible to calculate the adhesion coefficient α. With a channel radius of 100 μm and width of alloy of 412 μm, the adhesion coefficient is: $\alpha = 5.6 \times 10^6$ N.m^{-2}. This device can therefore withstand a maximum pressure difference of 24 MPa.

Sample no	0	1	2	3	4
Width of alloy (μm)	0	400	400	500	600
Opening pressure (kPa)	157	120	128	160	140

TABLE I: Opening pressure for different size of the alloy. Sample 0 corresponds to Cr and Cu layers with no alloy.

C. Opening pressure

When the ambient temperature is above the melting point of the alloy, this lasts becomes liquid. In this state, two forces oppose the pressure difference across the channel: the mechanical resistance of the chromium and copper layers, the tension of the air/melted alloy interface. The mechanical resistance of the chromium and copper layers is measured on a sample without the alloy part. The membrane is modeled by an homogeneous membrane clamped at its edges. From [10], the fracture strength is given by:

$$\sigma_f = \frac{3 \Delta P R_c^2}{4 t^2}, \tag{3}$$

where t is the thickness of the membrane. From the experiments, a membrane of radius 100 μm, thickness 400 nm is broken by a pressure difference $\Delta P = 157000$ Pa, which gives $\sigma_f = 7$ GPa. Equation 3 can be used to design the specific opening pressure of the valve by changing the thickness and radius of the membrane. The effect of the surface tension can be estimated by using the following formula:

$$\Delta P = 2 \frac{\sigma}{R_b},$$

with ΔP the over-pressure needed to create a gas bubble of radius R_b with an interfacial tension σ [11]. The tension of the alloy/air interface has been reported to be 0.55 N.m^{-1} [12]. With a bubble radius equal to the radius of the channel, the over-pressure to create the gas bubble is calculated to be only $\Delta P = 11000$ Pa and can be neglected.

Finally we compare the opening pressure for several devices with different size of solder. The radius of the channel is kept constant at 100 μm. The results are shown in Tab. I. We can see that the opening pressure is merely independent on the presence and size of the alloy part. The discrepancies between the opening pressures can be explained by the difference in the thickness of the chromium and copper layers deposited by sputtering.

D. Temperature sensitivity and time response

It is important to know the sensitivity of the opening with respect to temperature, i.e. if the device will

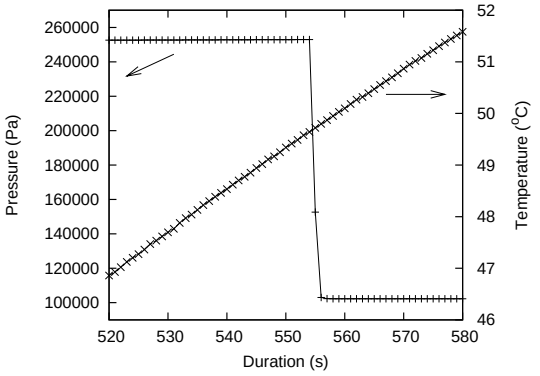

FIG. 5: Temperature sensitivity of the device. Input pressure and temperature as a function of time with increasing temperature. The output pressure is 101 kPa.

response quickly to a change in the ambient temperature and how different the opening temperature is from the melting temperature of the alloy.

The device is placed under a pressure difference of 1.5×10^5 Pa at 20 °C. The ambient temperature is then raised at a rate of 0.1 °C.s^{-1}. The temperature and input pressure in the device as a function of time are reported in Fig. 5. The drop in the input pressure indicates the opening of the valve and occurs at 49.7 °C. The melting point of the alloy is, according to the manufacturer, 47 °C. From this measurement we can deduce that the temperature sensitivity of the device is below 3 °C. Moreover, the device opens 33 s after the ambient temperature has reached 47 °C. From this we can deduce that the time response of the device is below this value. The experiment reported in Fig. 5 exhibits a combination of the temperature sensitivity and time response of the device. More accurate characterizations are needed in order to separate these two phenomenons. However, this experiment gives maximum limits for these two characteristics.

V. CONCLUSIONS

A novel one-shot valve using MEMS technologies has been presented. This device opens when the ambient temperature is above a set value defined by the design. It can be used for safety purpose in portable power devices such as portable fuel cells. Several characteristics have been presented as well as some models which allow for the design of the device. Future work includes more characterizations and new designs incorporating for example a micro-heater for on-demand triggering operation.

Acknowledgment

This work is supported by VLSI Design and Education Center (VDEC), the University of Tokyo, with the collaboration of CADENCE Corporation. We thank M. Yokoi and Nakakubo for their assistance in the use of the traction machine.

[1] D.J. Beebe, J.S. Moore, J.M. Bauer, Q. Yu, R.H. Liu, C. Devadoss, and B.-H. Jo. Functional hydrogel structures for autonomous flow control inside microfluidic channels. *Nature*, 404:588–590, 2000.

[2] A. Baldi, Y.D. Gu, P.E. Loftness, R.A. Siegel, and B. Ziaie. A hydrogel-actuated environmentally sensitive microvalve for active flow control. *J. Microelectromech. Syst.*, 12:613–621, 2003.

[3] L. Dong, A.K. Agarwal, D.J. Beebe, and H. Jiang. Adaptive liquid microlenses activated by stimulireponsive hydrogels. *Nature*, 442:551–554, 2006.

[4] P. Griss, Andersson H., and G. Stemme. Liquid handling using expandable microspheres. In *IEEE MEMS Conference*, pages 117–120, 2002.

[5] H.-D. Stockhausen, H. Seidelberger, G. Hau, and J. Hollmann. Safety device protecting against overpressure failure of a nuclear reactor pressure vessel. US Patent no. 5526385, 1994.

[6] P.M. Holmes. Thermally operated valve. US Patent no. 4313453, 1979.

[7] D. H. Gracias, J. Tien, T. L. Breen, C. Hsu, and G. M. Whitesides. Forming electrical network in three dimensions by self-assembly. *Science*, 289:1170–1172, 2000.

[8] A. Debray, T. Nakakubo, A. Yokoi, S. Mogi, K. Ueda, M. Shibata, S. Takeuchi, and H. Fujita. A micromachined safety valve for power applications with improved sealing. *J. Micromech. Microeng.*, 16:S240–S247, 2006.

[9] C.D. Ehrlich and J.A. Basford. Recommended practices for the calibration and use of leaks. *J. Vac. Sci. Technol. A*, 10(1):1–17, 1992.

[10] W.C. Young. *Roark's formulas on stress and strain.* McGraw-Hill international editions, 1989.

[11] K.J. Mysels. Improvements in the maximum-bubble-pressure method of measuring surface tension. *Langmuir*, 2:428–432, 1986.

[12] J. Lienemann, A. Greiner, J.G. Korvink, X. Xiong, Y. Hanein, and K.F. Böhringer. Modeling, simulation, and experimentation of a promising new packaging technology: Parallel fluidic self-assembly of microdevices. *Sensors Update 13*, pages 3–43, 2004.